2012

Multi-payload measurement of transverse velocity shears in the topside ionosphere

E. T. Lundberg
Cornell University

P. M. Kintner
Cornell University

Kristina A. Lynch
Dartmouth College, Kristina.A.Lynch@dartmouth.edu

M. R. Mella
Dartmouth College

Multi-payload measurement of transverse velocity shears in the topside ionosphere

E. T. Lundberg,[1,2] P. M. Kintner,[1] K. A. Lynch,[3] and M. R. Mella[3]

Received 26 October 2011; revised 13 December 2011; accepted 14 December 2011; published 12 January 2012.

[1] Using a multi-payload sounding rocket mission, we present the first direct measurement of velocity shear in the topside auroral ionosphere. In regions of large, ~200 mV/m, transient electric fields we directly measure differences in the plasma drift velocity. From these differences, shear frequencies reaching ±6Hz are measured. These directly measured shears are compared with the shear inferred from single payload measurements. It is shown this traditional measurement of shear overestimates the shear frequency by a factor of two for this event, highlighting the importance of the temporal component of near-DC electric field structures. Coincident with these strong fields and shears are enhanced emissions of broadband, extremely low frequency (BB-ELF) plasma waves, and a narrowband wave emission near the H^+-O^+ bi-ion resonant frequency. **Citation:** Lundberg, E. T., P. M. Kintner, K. A. Lynch, and M. R. Mella (2012), Multi-payload measurement of transverse velocity shears in the topside ionosphere, *Geophys. Res. Lett.*, *39*, L01107, doi:10.1029/2011GL050018.

1. Introduction

[2] Observations of inferred shear in transverse flows in the topside ionosphere associated with auroral activity have been reported for at least three decades [*Kelley and Carlson*, 1977], and in the auroral acceleration region slightly earlier [*Kintner*, 1976]. Units of velocity shear, $f_s = |\partial V_x/\partial x|$, are Hz, which is convenient for comparison between different space plasmas and with laboratory plasmas. Typical inferred shear frequencies measured in the auroral zone are of the order 0.1 Ω_i, where $\Omega_i = 2\pi f_{ci}$ is the ion cyclotron frequency (see review by *Amatucci* [1999]). The main drawback to these single point measurements is their assumption of stationarity in the plasma frame, i.e. that variations in the measured electric field are entirely due to the spacecraft passing through spatial structures. Using this assumption shear has been inferred by differencing subsequent electric field measurements and dividing by the distance the spacecraft traveled between each measurement. Often, this has been further simplified to the very rough approximation $f_s \simeq V_e^0/L$, where V_e^0 is the E × B drift velocity, and L is shear region scale size determined by the spacecraft velocity and traversal time.

[3] In their landmark paper, *Kindel and Kennel* [1971] predict the instability of O^+ and H^+ electrostatic ion cyclotron (EIC), and ion acoustic waves, due to field aligned currents in the topside auroral ionosphere. The EIC waves are distinguished by their structure at and near multiples of the ion gyrofrequencies which allows the waves to gyroresonantly interact with and heat ionospheric ions. This efficient heating gives this instability special importance and it has subsequently been termed the current driven electrostatic ion cyclotron (CDEIC) instability.

[4] There have been sounding rocket observations of plasma wave emissions with structure at or near multiples of Ω_{H^+} in the auroral ionosphere which have been identified as ion-Bernstein mode waves [*Mosier and Gurnett*, 1969; *Kintner et al.*, 1991]. Magnetospheric observations of H^+ cyclotron waves have been more common, and their growth has been attributed to inhomogeneities in the ion distribution functions [*Cattell and Hudson*, 1982; *Eliasson et al.*, 1994]. There have been less frequent reports of sounding rocket observations of O^+ gyroharmonic structure, which is difficult to capture due to Doppler spreading [*Kintner et al.*, 1989; *Bering et al.*, 1975]. There have been limited reports of wave emission at the ion-ion resonant frequencies [*Lund and LaBelle*, 1997]. On the other hand, BB-ELF waves are commonly observed on both sounding rockets, and satellites [*André et al.*, 1998], and are almost always associated with TAI [*Kintner et al.*, 1996; *Lynch et al.*, 2002; *Knudsen et al.*, 1998].

[5] A statistical study carried out by *André et al.* [1998] showed that auroral field aligned currents are generally too weak to directly destabilize the CDEIC which indicated the need for additional instabilities to explain the ubiquity of BB-ELF. A leading candidate for the generation of BB-ELF are inhomogeneous electric fields (velocity shear), which have been shown to excite ion-cyclotron waves, and have been termed the inhomogenous energy density driven instability (IEDDI) [*Ganguli et al.*, 1988]. It was shown by *Gavrishchaka et al.* [2000] that inhomogeneous parallel flow could generate ion-cyclotron waves in the auroral acceleration region. A second class of instabilities, due to current shear have been shown to destabilize ion-cyclotron waves via collisionless tearing mode instabilities, and are most recently referred to as current shear-driven instabilities (CSD) [*Seyler and Wu*, 2001]. The relationship between the fluctuating electric and magnetic fields in Alfvén waves, CSD instabilities, electron acceleration and BB-ELF plasma wave emission was made by *Seyler and Liu* [2007].

[6] In this letter we will use observations from a multi-payload auroral sounding rocket mission to present the first direct measurement of transverse shear in the transverse flow in the topside auroral ionosphere. The directly measured shears are compared to the traditional measurement of shear

[1]Department of Electrical and Computer Engineering, Cornell University, Ithaca, New York, USA.
[2]Now at The MITRE Corporation, Bedford, Massachusetts, USA.
[3]Department of Physics, Dartmouth College, Hanover, New Hampshire, USA.

0094-8276/12/2011GL050018

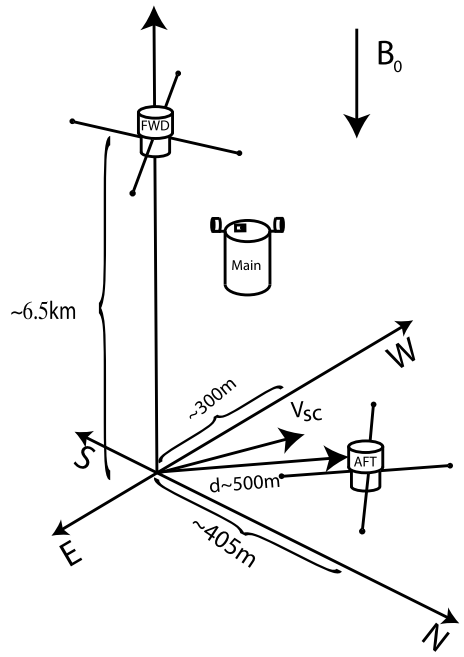

Figure 1. A cartoon illustrating the configuration of the payloads (not to scale), the coordinate systems, and the geometry of the shear measurement.

and shown to be a factor of two smaller. The largest shears are measured in the regions of largest fluctuating electric fields. Associated with these fluctuating fields and shears is increased BB-ELF plasma wave emission, and narrowband wave emission at 0.9 f_{cH^+}. During this same active region there may be evidence of transversely accelerated ions (TAI).

2. Cascades-2 Instrumentation

[7] The Cascades-2 sounding rocket was launched from Poker Flat Research Range (PFRR) at 11:04:00 UT on March 20th, 2009, into a pre-midnight Poleward Boundary intensification (PBI see *Mella et al.* [2011]). Early on the upleg, two Cornell Wire Boom Yo-yo (COWBOY) electric/magnetic field subpayloads with their spin axes aligned to $\mathbf{B}_0$ were ejected nearly parallel and anti-parallel to the spin axis from the main payload with a differential velocity of 15 m/s. Each COWBOY was equipped with a pair of crossed 12.14 m dipoles formed by 4.45 cm diameter spheres deployed at the ends of coaxial wire booms. Onboard GPS receivers ensured synchronous sampling between payloads and provided positioning with ~5 m accuracy [*Powell et al.*, 2002].

[8] Data presented herein were taken during a 12 s period on the downleg where the AFT payload traverses the altitude range from 450–433 km. The payloads' GPS positions and velocities were transformed into a magnetic Vertical-East-North coordinate system, where the x-axis is aligned opposite to the local magnetic field, the z-axis points toward the magnetic North pole and y-axis completes the right handed triad. Along the magnetic field, the FWD payload was 6250–6475 m above of AFT. In the plane perpendicular to $\mathbf{B}_0$, the AFT payload was 395–415 m North, and 273–323 m West of FWD, which formed an angle 52.5 degrees West of North that changed by less than half a degree over the selected time period. The magnitude of the inter-payload separation vector in the perpendicular plane, $d = |\mathbf{d}|$, went from 480 m to 525 m. The spacecraft velocity, v_{sc}, was 1470 m/s in the plane perpendicular to $\mathbf{B}_0$ which pointed 57.3 degrees West of North.

[9] We used a modified version of the filter/smoother described by *Humphreys et al.* [2005] to transform the raw, DC (0–1 kHz), electric field data into a frame whose axes are aligned parallel and perpendicular to the projection of the inter-payload separation vector into the plane perpendicular to $\mathbf{B}_0$. The relative positions of the payloads are shown in Figure 1.

3. Cascades-2 Data

[10] Figure 2b shows the despun DC electric field from the FWD (dashed) and AFT payloads (solid). Figure 2d shows the E-field power spectrum between 20 Hz-10 kHz. Figure 2a shows the field aligned electron count rate from 0–1 keV (swept every 8 ms). The "stripe" in the electron data at around 10 eV is an instrumental artifact. The fluctuating DC electric field reaches peak-to-peak values of ~330 mV/m. Coincident with these large electric fields is a series of highly field aligned suprathermal electron bursts (STEB). Both the fields and electrons are modulated at ~8 Hz, and the strong correlation between the DC electric fields and STEB is indicative of Alfvénic aurora. From the lower hybrid resonance (LHR) at ~6 kHz we obtain a rough density estimate of $1–2 \times 10^4$ cm^{-3}. (A more detailed density estimate will be presented later in the paper.) Magnetometer deflections of up to ~100 nt are observed indicating $|\delta E/\delta B|$ of $1–2 \times 10^6$ m/s which is on the order of the mass-density derived Alfvén velocity of 2.1×10^6 m/s. These magnetic field data are omitted due to our inability to achieve the sub-degree level attitude accuracy needed to accurately despin magnetometer data at these altitudes. Below f_{LH} there is evidence of increased BB-ELF activity up to ~1 kHz. Impulsive broadband features stretching from 20 *Hz–*f_{LH} indicate the possible presence of Lower-Hybrid Solitary Structures (LHSS) [*Kintner et al.*, 1992].

[11] From the despun DC electric field measurements, we can obtain the transverse plasma drift velocity, $\mathbf{V} = \mathbf{E} \times \mathbf{B}/|\mathbf{B}|^2$. To calculate shear, we approximate the spatial derivative with the finite difference $\partial V/\partial x \approx (V(x + d) - V(x))/d$, where x is the location of one payload and d is the interpayload separation distance. We assume perfect field-line mapping over the ~6.5 km parallel separation of the payloads and note that d is greater than both ion gyroradii (ρ_{o^+} = 22 m, ρ_{H^+} = 1.6 m), and the electron inertial length (λ_e = 42 m). We illustrate this assumption in Figure 1 which shows how we are projecting the FWD payload along the nearly vertical field lines to the altitude of the AFT payload, thereby assuming all measured electric field variations are due entirely to the payloads' perpendicular separation. The choice of a separation vector aligned coordinate system allows for observation of two components of the shear, the shear in the flow parallel and perpendicular to interpayload separation vector, and is shown in Figure 2c. A third measurement point would allow measurement of vorticity, $\nabla \times \mathbf{V}$, which quantifies both the degree of rotation and the magnitude of shear [*Chaston et al.*, 2010]. Since our two point finite difference approximation is first order it

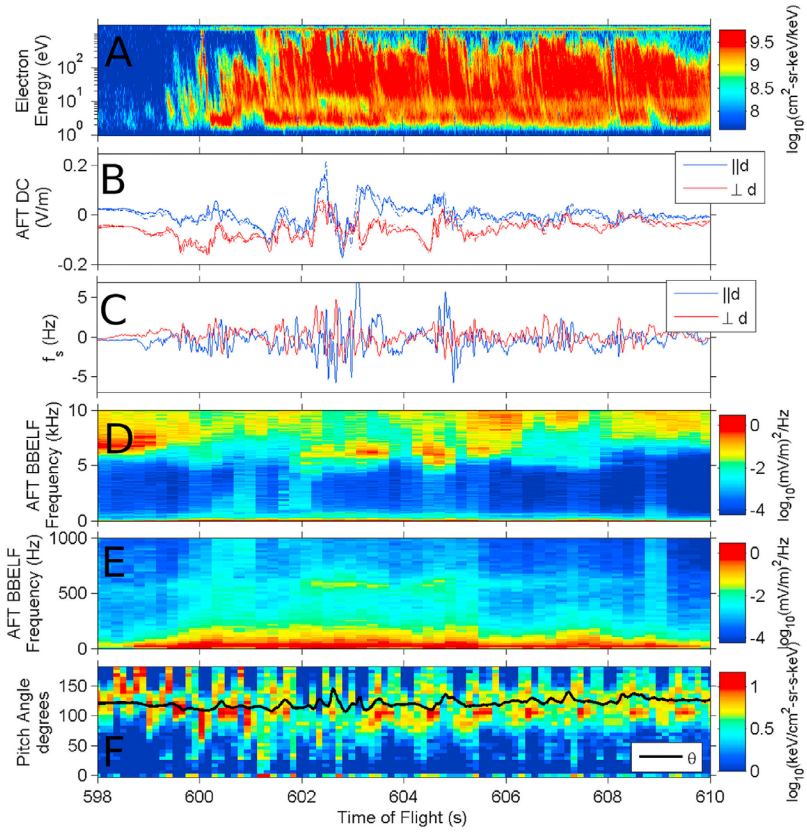

Figure 2. An overview of Cascades-2 measurements between 598 and 610 s. (a) Field aligned electrons between 0 and 1 keV. (b) DC Electric field measured by the AFT (solid) and FWD (dashed) payloads in a coordinate system whose axes are aligned (blue) and perpendicular (red) to the interpayload separation vector. (c) Shear measured by differencing multipoint electric field measurements. (d) VLF plasma waves measured on the AFT payload. (e) BB-ELF plasma waves measured on the AFT payload. (f) Pitch angle spectrogram measured on the main payload between 1.5 and 7.0 eV. The black line indicates the combined payload and plasma velocity ram direction.

will miss higher order spatial variations. This measurement also assumes there is no variation on scales less than the perpendicular separation of the two payloads. The highest measured shear frequency of 6 Hz corresponds to velocity differences of 3000 m/s and field differences of 150 mV/m. This analysis represents a fully spatial interpretation of these signals.

[12] Figure 2e displays the electric field power spectrum from 20 Hz-1 kHz from the 3–4 antenna baseline on the FWD payload. Between 20 Hz and 200 Hz there are increased BB-ELF emissions. In addition to enhanced BB-ELF emissions there is a narrow (∼80 Hz wide) emission around 600 Hz. This is approximately 0.9 × f_{cH^+} where f_{cH^+} = 736 Hz (for reference f_{cO^+} = 46 Hz). These narrowband waves are highly correlated with the regions of largest shear.

[13] Figure 2f shows the ion pitch angle spectrogram using the energy bins from 1.5 eV to 7.3 eV, where 0 is aligned to $\mathbf{B}_0$. The black line in Figure 2f corresponds to the ram direction of the combined payload velocity and plasma drift velocity given by the expression $\theta = \cos^{-1}(\mathbf{B}_0 \cdot \mathbf{v}_{rel}/(|\mathbf{B}_0||\mathbf{v}_{rel}|))$ and $\mathbf{v}_{rel} = \mathbf{v}_{sc} - \mathbf{v}_{\mathbf{E}\times\mathbf{B}}$. The ∼1 s periodicity in the color (count rate) of the ions is due to the rotation of payload in and out of this ram direction. The majority of the ions have pitch angles within ∼10 degrees of perpendicular. The bulk of the thermal population followed this ram direction throughout the flight; the enhancements seen at closer to 90 deg pitch angle may be indicative of local transverse heating. Ion temperatures during the time shown, including the times of strongest shears, were in the 1–2 eV range, hotter than in undisturbed portions of the flight (where they were often below 1 eV) but not as hot as during other arcs, where they reached up above 2 eV. Absolute temperatures of ionospheric ions, however, are as much a function of heating duration as of the strength of the heating process [*Andre and Yau*, 1997]. The thermal fluxes saturated the pitch angle imaging at the core of the distribution, so only the tail of the thermal population could be imaged. There was no mass discrimination on the ion measurements.

[14] Figure 3 shows the AFT VLF and HF (1 kHz-2.4 MHz) power spectra during the active period at t = 603.4 s in blue. For comparison, we include similar data from t = 325 s, a significantly less active period of the flight, when the payload was on the upleg and at an altitude of 518 km. In the active region, we measure a plasma frequency of 1.158 MHz, which is lower than the electron cyclotron frequency f_{ce} of 1.34 MHz, and therefore lower than the upper hybrid frequency. From this we determine the plasma density to be 1.34 × 10^4 cm^{-3}. Assuming a two component local plasma whose species are O^+ and H^+, an f_{LH} of 6002 Hz indicates a 2.5% H^+ concentration. By repeating this analysis for a number of cases on both payloads and at numerous times we find the H^+ concentration to

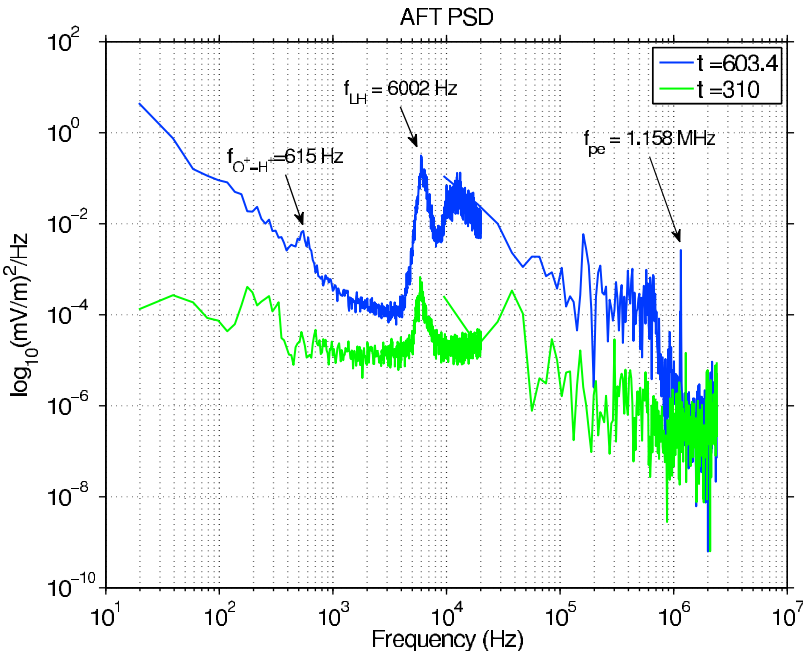

Figure 3. Power spectra of the VLF and HF channels indicating lower-hybrid, BB-ELF, bi-ion resonance, and langmuir waves.

be between 2–3% for the entire region of narrowband wave emission. The existence of a second ionic component introduces two new frequencies of interest, the bi-ion resonance and cutoff frequencies [*Buchsbaum*, 1960]. For a 2.5% H^+, 97.5% O^+ plasma, the bi-ion resonance frequency is 615 Hz [*Smith and Brice*, 1964]. In addition to the EIC modes and the bi-ion resonances, the other electrostatic plasma wave mode below f_{LH} is the ion-acoustic mode, which is less likely to be unstable in the topside auroral ionosphere [*Kindel and Kennel*, 1971]. An alternative interpretation of these narrowband waves is that they are spatial structures of 2.4 m Doppler shifted by the ∼1500 m/s spacecraft velocity perpendicular to the magnetic field ($2\pi f_{doppler} = \mathrm{v}_\perp^{s/c}\,\mathrm{k}$).

4. Discussion

[15] The choice of a separation vector aligned coordinate system and the near collinearity of the d and $\mathrm{v}_\perp^{s/c}$ allows for a comparison between traditional methods of measuring shear. We apply the traditional measurement of shear [e.g., *Kelley and Carlson*, 1977; *Earle et al.*, 1989] to our largest peak-to-peak DC electric field variation. This variation of 336 mV/m, in the direction aligned to the interpayload separation vector, was recorded over .43 s at 602 s into the flight, while the velocity of the payload perpendicular to $\mathbf{B}_0$ was ∼1500 m/s. From these parameters we obtain a shear frequency estimate of ∼12Hz. This is significantly higher than our directly measured shears indicating that a significant portion of the measured electric field fluctuations must be temporal, i.e., the slope in the measured electric field is due both to the spacecraft's motion through a structured electric field and that structured field's dynamic evolution and propagation past the spacecraft. In both directions the shear is both positive and negative, indicating passage through spatially oscillatory structures.

[16] *Ganguli et al.* [1994] outline a hierarchy of microinstabilities that can be triggered by velocity shear. Our measured shear frequency of $\sim.125\Omega_{cO^+}$ falls between the IEDDI case, where $\omega_s \sim \omega_{Ci}$, and the Kelvin-Helmholtz (KH) instability case, where $\omega_s \ll \omega_{Ci}$. IEDDI mechanisms have been shown to produce EIC type waves which are broadband [*Ganguli et al.*, 1994]. In general, the response of the plasma is to dissipate shears, so although we observe shear frequencies below the IEDDI excitation threshold, there could be shears above it prior to our measurement time [*Romero and Ganguli*, 1993]. In certain cases, simulation has shown that the non-linear evolution and steepening of the KH instability can develop small scale regions of intense shear which can then excite IEDDI [*Ganguli et al.*, 1994]. The general IEDDI theory has been extended to multicomponent plasmas and it has been shown that this destabilizes plasma waves at 0.9–0.95 times the minority species cyclotron frequency [*Gavrishchaka et al.*, 1997], strongly suggesting our observed narrowband plasma waves are IEDDI driven.

[17] In the CSD instabilities of *Liu et al.* [2006], regions of largest current shear correspond to regions of largest DC electric field. Because our measured regions of highest shear are collocated with the most intense DC electric fields, we cannot discount CSD mechanisms. We illustrate the difficulty of distinguishing between the IEDDI and CSD modes with a simple example. Imagine a 1 Hz, inertial Alfvén wave with a perpendicular wavelength of 1000 m, detected by measuring a δE of 100 mV/m. On scales of 500 m, shear frequencies of up to 10 Hz would be measured, and exist, in the region between the peak and trough of this wave. The growth rate of the IEDDI in this situation would be on the order of $0.01–0.05\Omega_{O^+}^{-1}$, which is close to the 1 s period of the Alfvén wave, and would therefore be slightly unstable. Following the inertial Alfvén wave dispersion relation, $|\frac{\delta E}{\delta B}| = V_a\sqrt{1+k_\perp^2\lambda_e^2}$, δB in this scenario would be 50 nT. Since there is no excitation threshold for CSD, the very existence

of an Alfvén aurora is sufficient to destabilize it. Given its lack of excitation threshold, we believe the CSD instability is a more likely candidate to explain the observed BB-ELF. This may explain why we observe BB-ELF waves over the entire active region rather than just the region of highest shears. However, given the complexity of Alfvénic aurora, either the CSD or the IEDDI could be significant, and we believe the best explanation for the observed BB-ELF may be a combination of both.

[18] In conclusion, we present the first direct measurement of velocity shear in the topside auroral ionosphere above an active auroral display, and measure shear frequencies in excess of 6 Hz. This directly measured shear is a factor of two less than traditional measurement techniques would imply applied to the same data set, indicating the need to consider propagation effects when interpreting DC electric field structures. We do not attempt to explain the mechanism that supports these differences and instead focus on the microphysics driven by them. These shears were measured in regions of intense, fluctuating DC electric fields. High shear regions ($f_s > 4$) are collocated with BB-ELF plasma waves, and narrowband low frequency plasma waves occurring at the bi-ion resonance frequency. The existence of these narrowband waves are highly likely due to the IEDDI. The plasma wave data implies the existence of a minority ionic constituent indicating the need to include them in future simulation and modeling work.

[19] **Acknowledgments.** We would like to thank Charles Seyler and David Hysell for helpful discussions. This research was funded by NASA grant NNX07AN38G.

[20] The Editor thanks two anonymous reviewers for their assistance in evaluating this paper.

References

Amatucci, W. E. (1999), Inhomogeneous plasma flows: A review of in situ observations and laboratory experiments, *J. Geophys. Res.*, *104*, 14481–14504, doi:10.1029/1998JA900098.

Andre, M., and A. Yau (1997), Theories and observations of ion energization and outflow in the high latitude magnetosphere, *Space Sci. Rev.*, *80*, 27–48, doi:10.1023/A:1004921619885.

André, M., P. Norqvist, L. Andersson, L. Eliasson, A. I. Eriksson, L. Blomberg, R. E. Erlandson, and J. Waldemark (1998), Ion energization mechanisms at 1700 km in the auroral region, *J. Geophys. Res.*, *103*, 4199–4222, doi:10.1029/97JA00855.

Bering, E. A., M. C. Kelley, and F. S. Mozer (1975), Observations of an intense field-aligned thermal ion flow and associated intense narrow band electric field oscillations, *J. Geophys. Res.*, *80*, 4612–4620, doi:10.1029/JA080i034p04612.

Buchsbaum, S. J. (1960), Resonance in a plasma with two ion species, *Phys. Fluids*, *3*, 418–420, doi:10.1063/1.1706052.

Cattell, C., and M. Hudson (1982), Flute mode waves near the lower hybrid frequency excited by ion rings in velocity space, *Geophys. Res. Lett.*, *9*, 1167–1170, doi:10.1029/GL009i010p01167.

Chaston, C. C., K. Seki, T. Sakanoi, K. Asamura, and M. Hirahara (2010), Motion of aurorae, *Geophys. Res. Lett.*, *37*, L08104, doi:10.1029/2009GL042117.

Earle, G. D., M. C. Kelley, and G. Ganguli (1989), Large velocity shears and associated electrostatic waves and turbulence in the auroral F region, *J. Geophys. Res.*, *94*, 15,321–15,333, doi:10.1029/JA094iA11p15321.

Eliasson, L., M. André, A. Eriksson, P. Norqvist, O. Norberg, R. Lundin, B. Holback, H. Koskinen, H. Borg, and M. Boehm (1994), Freja observations of heating and precipitation of positive ions, *Geophys. Res. Lett.*, *21*, 1911–1914, doi:10.1029/94GL01067.

Ganguli, G., Y. C. Lee, and P. J. Palmadesso (1988), Kinetic theory for electrostatic waves due to transverse velocity shears, *Phys. Fluids*, *31*, 823–838, doi:10.1063/1.866818.

Ganguli, G., M. J. Keskinen, H. Romero, R. Heelis, T. Moore, and C. Pollock (1994), Coupling of microprocesses and macroprocesses due to velocity shear: An application to the low-altitude ionosphere, *J. Geophys. Res.*, *99*, 8873–8889, doi:10.1029/93JA03181.

Gavrishchaka, V. V., M. E. Koepke, and G. I. Ganguli (1997), Ion cyclotron modes in a two-ion-component plasma with transverse-velocity shear, *J. Geophys. Res.*, *102*, 11,653–11,664, doi:10.1029/97JA00639.

Gavrishchaka, V. V., G. I. Ganguli, W. A. Scales, S. P. Slinker, C. C. Chaston, J. P. McFadden, R. E. Ergun, and C. W. Carlson (2000), Multiscale coherent structures and broadband waves due to parallel inhomogeneous flows, *Phys. Rev. Lett.*, *85*, 4285–4288, doi:10.1103/PhysRevLett.85.4285.

Humphreys, T. E., M. L. Psiaki, E. M. Klatt, S. P. Powell, and P. M. Kintner (2005), Magnetometer-based attitude and rate estimation for spacecraft with wire booms, *J. Guidance Control Dyn.*, *28*, 584–593.

Kelley, M. C., and C. W. Carlson (1977), Observations of intense velocity shear and associated electrostatic waves near an auroral arc, *J. Geophys. Res.*, *82*, 2343–2348, doi:10.1029/JA082i016p02343.

Kindel, J. M., and C. F. Kennel (1971), Topside current instabilities, *J. Geophys. Res.*, *76*, 3055–3078, doi:10.1029/JA076i013p03055.

Kintner, P. M., Jr. (1976), Observations of velocity shear driven plasma turbulence, *J. Geophys. Res.*, *81*, 5114–5122, doi:10.1029/JA081i028p05114.

Kintner, P. M., W. Scales, J. Vago, R. Arnoldy, G. Garbe, and T. Moore (1989), Simultaneous observations of electrostatic oxygen cyclotron waves and ion conics, *Geophys. Res. Lett.*, *16*, 739–742, doi:10.1029/GL016i007p00739.

Kintner, P. M., J. Vago, W. Scales, A. Yau, B. Whalen, R. Arnoldy, and T. Moore (1991), Harmonic H(+) gyrofrequency structures in auroral hiss observed by high-altitude auroral sounding rockets, *J. Geophys. Res.*, *96*, 9627–9638, doi:10.1029/91JA00563.

Kintner, P. M., J. Vago, S. Chesney, R. L. Arnoldy, K. A. Lynch, C. J. Pollock, and T. E. Moore (1992), Localized lower hybrid acceleration of ionospheric plasma, *Phys. Rev. Lett.*, *68*, 2448–2451, doi:10.1103/PhysRevLett.68.2448.

Kintner, P. M., J. Bonnell, R. Arnoldy, K. Lynch, C. Pollock, and T. Moore (1996), SCIFER-Transverse ion acceleration and plasma waves, *Geophys. Res. Lett.*, *23*, 1873–1876, doi:10.1029/96GL01863.

Knudsen, D. J., J. H. Clemmons, and J.-E. Wahlund (1998), Correlation between core ion energization, suprathermal electron bursts, and broadband ELF plasma waves, *J. Geophys. Res.*, *103*, 4171–4186, doi:10.1029/97JA00696.

Liu, K., C. E. Seyler, and T. Xu (2006), Particle-in-cell simulations of current shear-driven instabilities and the generation of broadband ELF fluctuations, *J. Geophys. Res.*, *111*, A11307, doi:10.1029/2006JA011858.

Lund, E. J., and J. LaBelle (1997), On the generation and propagation of auroral electromagnetic ion cyclotron waves, *J. Geophys. Res.*, *102*, 17,241–17,254, doi:10.1029/97JA01455.

Lynch, K. A., J. W. Bonnell, C. W. Carlson, and W. J. Peria (2002), Return current region aurora: $E_{\parallel}$, j_x, particle energization, and broadband ELF wave activity, *J. Geophys. Res.*, *107*(A7), 1115, doi:10.1029/2001JA900134.

Mella, M. R., K. A. Lynch, D. L. Hampton, H. Dahlgren, P. M. Kintner, M. Lessard, D. Lummerzheim, E. T. Lundberg, M. J. Nicolls, and H. C. Stenbaek-Nielsen (2011), Sounding rocket study of two sequential auroral poleward boundary intensifications, *J. Geophys. Res.*, *116*, A00K18, doi:10.1029/2011JA016428.

Mosier, S. R., and D. A. Gurnett (1969), Ionospheric observation of VLF electrostatic noise related to harmonics of the proton gyrofrequency, *Nature*, *223*, 605–606, doi:10.1038/223605a0.

Powell, S. P., M. E. Klatt, and P. M. Kintner (2002), Plasma wave interferometry using GPS position and timing on a formation of three sub-orbital payloads, paper presented at ION GPS 2002, Inst. of Nav., Portland, Oreg.

Romero, H., and G. Ganguli (1993), Nonlinear evolution of a strongly sheared cross-field plasma flow, *Phys. Fluids B*, *5*, 3163–3181, doi:10.1063/1.860653.

Seyler, C. E., and K. Liu (2007), Particle energization by oblique inertial Alfvén waves in the auroral region, *J. Geophys. Res.*, *112*, A09302, doi:10.1029/2007JA012412.

Seyler, C. E., and K. Wu (2001), Instability at the electron inertial scale, *J. Geophys. Res.*, *106*, 21,623–21,644, doi:10.1029/2000JA000410.

Smith, R. L., and N. Brice (1964), Propagation in multicomponent plasmas, *J. Geophys. Res.*, *69*, 5029–5040, doi:10.1029/JZ069i023p05029.

P. M. Kintner and E. T. Lundberg, Department of Electrical and Computer Engineering, Cornell University, Rhodes Hall 301, Ithaca, NY 14850, USA. (etl22@cornell.edu)

K. A. Lynch and M. R. Mella, Department of Physics, Dartmouth College, Hanover, NH 03755, USA.